Available online at www.sciencedirect.com
ScienceDirect
Phytochemistry 67 (2006) 2550–2560
PHYTOCHEMISTRY
www.elsevier.com/locate/phytochem

Hyperforin and its analogues inhibit CYP3A4 enzyme activity

Ju-young Lee [a], Rujee K. Duke [b], Van H. Tran [a], James M. Hook [c], Colin C. Duke [a,*]

[a] *Pharmaceutical Chemistry, Faculty of Pharmacy, University of Sydney, Building A15, Science Road, Sydney, NSW 2006, Australia*
[b] *Department of Pharmacology, University of Sydney, NSW, Australia*
[c] *NMR Facility, School of Chemistry, University of New South Wales, NSW, Australia*

Received 11 July 2006; received in revised form 13 September 2006

Abstract

Literature indicates that herb–drug interaction of St. John's wort is largely due to increased metabolism of the co-administered drugs that are the substrates of cytochrome P450 (CYP) 3A4 enzyme, alteration of the activity and/or expression of the enzyme. The major St. John's wort constituents, acylphloroglucinols, were evaluated for their effects on CYP3A4 enzyme activity to investigate their roles in herb–drug interaction. Hyperforin and four oxidized analogues were isolated from the plant and fully characterized by mass spectral and NMR analysis. These acylphloroglucinols inhibited activity of CYP3A4 enzyme potently in the fluorometric assay using the recombinant enzyme. Furoadhyperforin (IC_{50} 0.072 μM) was found to be the most potent inhibitor of CYP3A4 enzyme activity, followed by furohyperforin isomer 1 (IC_{50} 0.079 μM), furohyperforin isomer 2 (IC_{50} 0.23 μM), hyperforin (IC_{50} 0.63 μM) and furohyperforin (IC_{50} 1.3 μM). As the acylphloroglucinols are potent inhibitors of the CYP3A4 enzyme, their modulation of the enzyme activity is unlikely to be involved in increased drug metabolism by St. John's wort.

Keywords: St. John's wort; Acylphloroglucinols; Hyperforin; Furohyperforin; Furoadhyperforin; NMR; MS and CYP3A4 enzyme

1. Introduction

St. John's wort preparation is the most widely used herbal medicine for the treatment of mild-to-moderate depression (Josey and Tackett, 1999). The preparation has become an alternative to synthetic antidepressants because of comparable clinical efficacy while lacking major side effects (Schrader, 2000; Woelk, 2000; Lecrubier et al., 2002; Schulz, 2006; Lawvere and Mahoney, 2005). In 2001, St. John's wort was the leading treatment for depression, outselling fluoxetine (Prozac®) by a factor of four in Germany (Di Carlo et al., 2001). Since reports of adverse herb–drug interaction, the sale of the St. John's wort preparations has dropped sharply. In USA, sales peaked at $300 million in 1998 and decreased to $9 million in 2004–2005 (Blumenthal, 2005).

St. John's wort preparation is an over-the-counter product for the treatment of mild-to-moderate depression. However, multiple cases of interactions with conventional medications have limited the safe use of St. John's wort (Ernst, 1999). St. John's wort has been shown to lower the blood concentrations of a large number of concomitant medications including cyclosporine, indinavir and oral contraceptives (Breidenbach et al., 2000; Mai et al., 2000; Piscitelli et al., 2000; Hall et al., 2003).

CYP3A4 enzyme metabolises the majority of the drugs used clinically (~60%) and therefore is frequently implicated in herb–drug interactions either by alteration of the activity and/or expression of the enzyme (Guengerich, 1997). Evidence in the literature indicates that clinical herb–drug interaction of St. John's wort is mainly due to induction of CYP3A4 enzyme (Mueller et al., 2006; Markowitz et al., 2003; Wang et al., 2001; Roby et al., 2000; Mannel, 2004).

St. John's wort preparations consist of the leaves and flowering tops of *Hypericum perforatum* L. The prepara-

* Corresponding author. Tel.: +61 2 9351 2321; fax: +61 2 9351 4391.
E-mail address: colind@pharm.usyd.edu.au (C.C. Duke).

0031-9422/$ - see front matter © 2006 Elsevier Ltd. All rights reserved.
doi:10.1016/j.phytochem.2006.09.018

tion contains several classes of compounds including naphthodianthrones (hypericin, pseudohypericin), acylphloroglucinols (hyperforin, adhyperforin), flavonols (quercetin, kaempferol), flavonol glycosides (quercetrin, rutin), biflavones (amentoflavone, biapigenin), and xanthones (1,3,6,7-tetrahydroxy-xanthone) (Nahrstedt and Butterweck, 1997). Hypericin, flavonoids and hyperforin have been suggested as the constituents contributing to the antidepressant activity of St. John's wort (Cott, 1997; Butterweck et al., 2003; Calapai et al., 2001; Müller, 2003).

Hyperforin was shown to potently block serotonin reuptake into the presynaptic nerve endings in rat synaptosomal preparations with an IC_{50} value of 0.2 μM (Müller, 2003; Chatterjee et al., 1998; Keller et al., 2003), whereas the oxidized hyperforin analogues were much less potent (IC_{50} values >20 μM) (Verotta et al., 2002; Verotta et al., 2000). These findings suggest that hyperforin has higher efficacy as an antidepressant than the oxidized analogues.

Hyperforin inhibited the activity of CYP3A4 enzyme with an IC_{50} of 2.3 μM in the testosterone 6β-hydroxylase assay (Obach, 2000). However, little is known about its oxidized analogues in the modulation of CYP3A4 enzyme activity. In this study, hyperforin and its oxidized analogues (Fig. 1) were isolated and fully characterized by mass spectra and NMR (600 MHz) and examined for the modulation of CYP3A4 enzyme activity.

2. Results and discussion

2.1. Characterization of hyperforins

Hyperforin and its analogues were characterized based on their mass spectral, ^1H and ^{13}C NMR data. Homonuclear and heteronuclear 2D-NMR including COSY, TOCSY, ^1H–^{13}C HSQC and ^1H–^{13}C HMBC were also employed to assign the chemical shifts of these compounds. The NMR and mass spectra of the isolated hyperforin and its analogue furohyperforin were consistent with the published data (Cui et al., 2004; Orth et al., 1999; Verotta et al., 1999; Wang et al., 2004; Fuzzati et al., 2001). The spectra of other hyperforin analogues including furoadhyperforin, furohyperforin isomer 1 and furohyperforin isomer 2 exhibited resonances consistent with the published partial NMR spectra (Vugdelija et al., 2000; Wolfender et al., 2003).

2.2. Mass spectra of hyperforin and its oxidized analogues

The electrospray ionization (ESI) spectrum of hyperforin (Table 1) showed a protonated molecular ion at *m/z* 537 and a base peak at *m/z* 505 corresponding to a loss of dimethylketene [O=C=C$(CH_3)_2$] from the K^+ adduct of hyperforin. Hyperforin exhibited moderate intensity ions at *m/z* 491 and 469 corresponding to the loss of an isoprene unit (2-methyl-1,3-butadiene, −68 amu) from $[M+Na]^+$ and $[M+H]^+$, respectively, and *m/z* 477 and 411 corresponding to the loss of 2-methyl-2,4-pentadiene (−82 amu) from $[M+Na]^+$ and the loss of isobutene plus dimethylketene (−126 amu) from $[M+H]^+$, respectively. The ion at *m/z* 413 which corresponded to a loss of an isobutene unit from *m/z* 469 was also observed.

Furohyperforin gave a much simpler ESI spectrum than its parent compound hyperforin. Furohyperforin exhibited the protonated molecular ion at *m/z* 553 as the base peak and a weak peak at *m/z* 535 corresponding to the loss of H_2O from $[M+H]^+$as well as two moderate intensity ions at *m/z* 349 $[M+H-204]^+$ and *m/z* 293 $[M+H-204-56]^+$. The ion at *m/z* 349 corresponded to the elimination of the olefin $C_{15}H_{24}$ from the cyclohexanone part of the bicyclic structure (Fuzzati et al., 2001) from protonation at the C-9 carbonyl, and *m/z* 293 a loss of isobutene from the isoprene unit at C-8. $[M+H-204]^+$ and $[M+H-204-56]^+$ appear to be characteristic of oxidized hyperforin with a free C-8 isoprene unit and C-9 carbonyl including furohyperforin (*m/z* 349 and 293) and furoadhyperforin (*m/z* 363 and 307).

The spectra of furohyperforin isomers 1 and 2 were similar. Both showed a protonated molecular ion at *m/z* 553 as the base peak and a prominent Na^+ adduct at *m/z* 575, and moderate intensity ions at *m/z* 485 and 465 corresponding to the respective loss of isoprene (−68 amu) and dimethylketene plus H_2O (−88 amu) from $[M+H]^+$. The only significant difference in the spectra of the two isomers was the intensity of the peak at *m/z* 485 which was approximately doubled in isomer 2. In contrast, the spectrum of furoadhyperforin was distinctly different from the other furohyperforins in this study exhibiting Na^+ adduct ion at *m/z* 589 as the base peak and a moderate intensity protonated molecular ion at *m/z* 567. The spectrum also showed a weak K^+ adduct at *m/z* 605 and a weak ion at *m/z* 521 corresponding to the loss of the isoprene unit from $[M+Na]^+$.

2.3. NMR of hyperforin and its oxidized analogues

Hyperforin and its homologue adhyperforin exhibited broad peaks in the ^1H NMR spectra and poor resolution of ^{13}C NMR signals (Verotta, 2003; Maisenbacher and Kovar, 1992) due to slow equilibration between the tautomers of the β-dicarbonyl system. The β-dicarbonyl moiety, which is stabilized in MeOH (Cui et al., 2004), is also responsible for the reactivity of hyperforin and adhyperforin. We also found that the ^1H NMR signals of hyperforin were sharper in CD_3OD than in the other solvents and the ^{13}C NMR had to be carried out in CD_3OD to avoid decomposition. Hyperforin analogues lacking the β-dicarbonyl moiety have greater stability than hyperforin, consistent with the findings of others (Verotta et al., 2002; Verotta et al., 1999; Vugdelija et al., 2000; Wolfender et al., 2003). The analogues exhibited better resolution of spectra in $CDCl_3$ and did not require stabilization by a protic solvent such as CD_3OD. These observations strongly indicate that the β-dicarbonyl system in

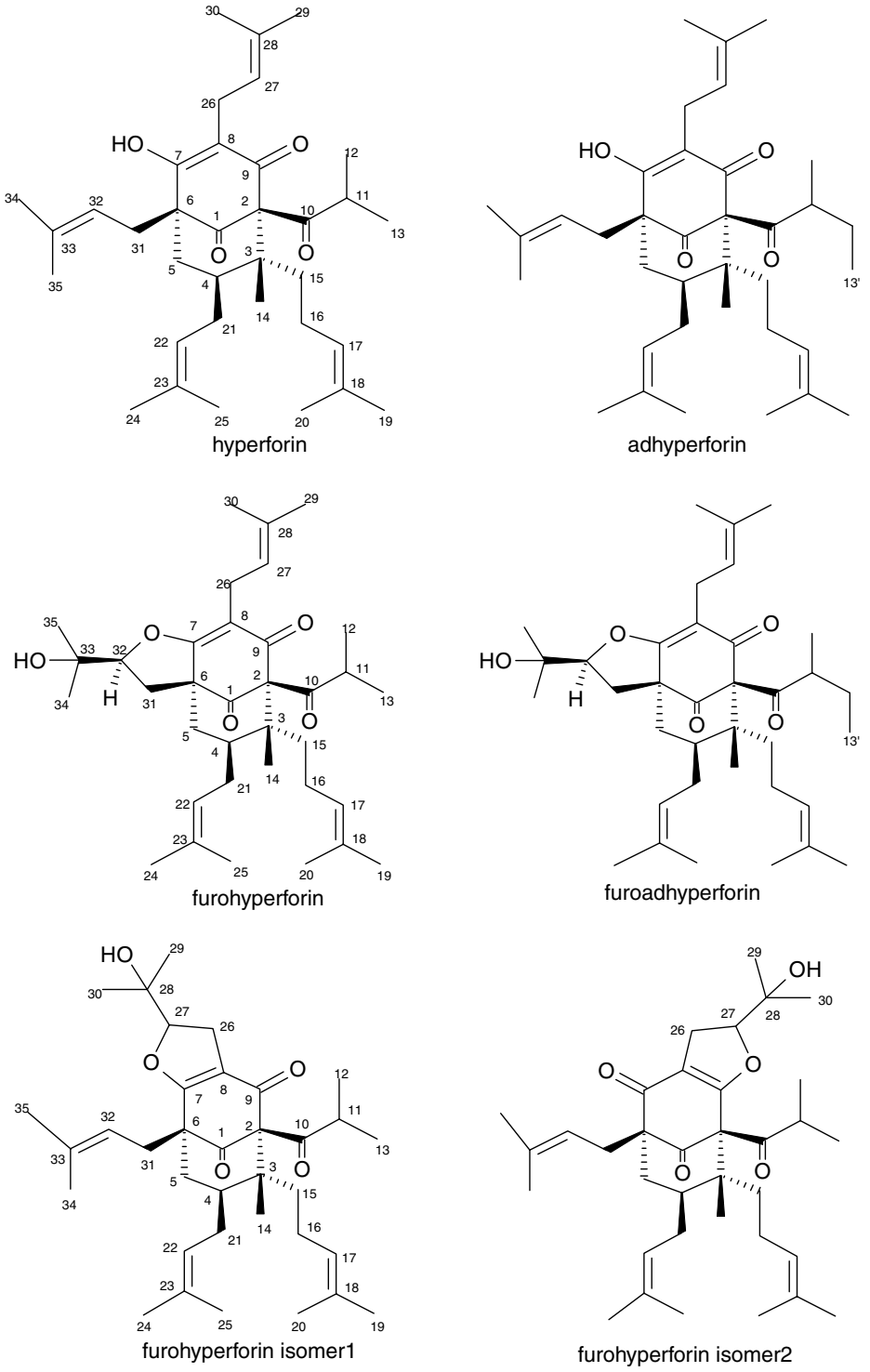

Fig. 1. The structures of hyperforin and its analogues.

Table 1
MS of hyperforin and its oxidized analogues

Compounds	MS ion peaks
Hyperforin	m/z 537 $[M+H]^+$ (18%), 505 (100%), 491 (37%), 481 (8%), 477 (40%), 469 (16%), 453 (9%), 413 (13%), 411 (16%)
Furohyperforin	m/z 553 $[M+H]^+$ (100%), 535 (11%), 349 (29%), 293 (28%)
Furoadhyperforin	m/z 605 $[M+K]^+$ (10%), 589 $[M+Na]^+$ (100%), 567 $[M+H]^+$ (22%), 521 (5%), 499 (2%), 453 (2%), 363 (2%), 307 (2%), 205 (2%)
Furohyperforin isomer 1	m/z 591 $[M+K]^+$ (7%), 575 $[M+Na]^+$ (25%), 553 $[M+H]^+$ (100%), 485 (12%), 465 (12.5%), 427 (4%), 293 (5%), 183 (2%)
Furohyperforin isomer 2	m/z 575 $[M+Na]^+$ (38%), 553 $[M+H]^+$ (100%), 485 (29%), 465 (11%), 427 (9%), 293 (8%)

hyperforin is stabilized in an enol form by hydrogen bonding with methanol.

Acylphloroglucinols display the characteristic ^{1}H NMR resonances that include the methyl signals of the isopropyl chain and the prenyl side chains (0.8–1.2 ppm and 1.2–1.8 ppm, respectively) and the olefinic resonances (4.5–5 ppm). The major differences in the ^{1}H and ^{13}C NMR spectra of hyperforin and the oxidized analogues were the signals belonging to the furan ring derived from the oxidation of one of the prenyl chains and the absence of the signals belonging to freely rotating prenyl side chain from which the furan ring was derived. Furohyperforin and furoadhyperforin displayed the resonances of C-6 and C-7 tetrahydro furan ring and the absence of the resonances of the freely rotating C-6 prenyl side chain. Furohyperforin isomers 1 and 2 exhibited the resonances belonging to the dihydro furan ring on C-7, C-8 and on C-8, C-9, respectively, and the resonances belonging to the freely rotating C-8 prenyl side chain were absent.

2.3.1. NMR of hyperforin

A systematic difference of approximately 0.1 ppm was observed in the ^{1}H NMR spectra of hyperforin (Table 2) when compared to the published data (Cui et al., 2004). This may be attributed to different concentrations of hyperforin as the same chemical shift reference was used in both studies. Within the ^{13}C NMR spectra, there are distinct non-systematic differences which are particularly noticeable in the ^{13}C chemical shifts of the atoms of the central ring C-1, C-6 to C-10, which may be ascribed to the hyperforin undergoing keto-enol equilibration at the higher concentration. This fluxional behavior of the central ring then may be transferred to the pendant isoprenoid arms to various extents such that differences in chemical shifts are noticeable at C-17, C-18, C-27, C-28 and C-32.

2.3.2. Furohyperforin and hyperforin

Furohyperforin is the major mono-oxidized derivative of hyperforin. Furohyperforin displayed a number of significant differences in the ^{1}H NMR spectrum (Table 3) compared with the parent compound hyperforin (Table 2). For example, the allylic CH_2 of the freely rotating C-6 prenyl side chain in hyperforin appears as two pairs of doublet of doublets, H-31α at δ2.41 ($J = 7.0$ and 14.6 Hz) and H-31β at δ2.51 ($J = 6.7$, 14.7 Hz), whereas the furan methylene resonances in furohyperforin appear as two pairs of doublet of doublets but clearly different, H-31α at δ2.65 ($J = 10.8$ and 13.0 Hz) and H-31β at δ1.76 ($J = 5.6$, 13.0 Hz). These differences in the couplings between the methylene protons and H-5 and to a lesser extent H-32 in hyperforin and furohyperforin indicate that incorporation of the methylene group into the rigid furan ring structure has resulted in considerable changes in the orientation of the protons involved. Minor differences observed for H-4, H-15 and H-21 in the hyperforin and furohyperforin spectra arise from conformational changes in the different solvents.

Table 2
NMR data of hyperforin

Position	Hyperforin		
	δ_H (J in Hz)	δ_C	HMBC
1	–	208.82	31
2	–	82.74	
3	–	49.54	
4	1.73, *m*	43.1	2, 3, 4, 5, 14, 15, 21, 22
5	1.91, *m*	40.8	
6	–	–	
7	–	–	
8	–	122.1	
9	–	–	
10	–	211.7	12, 13
11	2.10, *br*	43.0	10, 12, 13
12	1.03, *br*	21.99	10, 11, 13
13	1.09, *d* (6.7)	20.85	10, 11, 12
14	0.98, *s*	15.3	2, 3, 4, 15
15	1.68, *m*	37.88	2, 3, 4, 16, 17
16	1.74, *m* 2.06, *m*	28.62	3, 15, 17, 18
17	4.96, *t* (6.5)	120.85	15, 19, 20
18	–	134.69	
19	1.69, *s*	25.90	17, 18, 20
20	1.63, *s*	17.84	17, 18, 19
21	1.91, *m* 1.97, *m*	25.43	3, 4, 5, 22, 23
22	5.01, *tquin.* (7.3, 1.5)	126.05	4, 24, 25
23	–	131.81	
24	1.66, *s*	25.98	22, 23, 25
25	1.59, *s*	18.1	22, 23, 24
26	3.14, *dd* (7.2, 14.6) 3.09, *br*	22.50	7, 8, 9, 27, 28, 29
27	5.10, *tquin.* (7.2, 1.5)	122.54	8, 26, 29, 30
28	–	133.58	26, 27
29	1.646, *s*	26.16	27, 28, 30
30	1.71, *s*	18.15	27, 28, 29
31	2.41, *dd* (7.0, 14.6) 2.51, *dd* (6.7, 14.7)	30.70	1, 5, 6, 7, 32, 33
32	4.99, *br t* (7.8)	123.74	6, 34, 35
33	–	134.25	
34	1.69, *s*	26.05	32, 33, 35
35	1.585, *s*	18.25	32, 33, 34

Measured at 600 MHz (^{1}H) and 150 MHz (^{13}C) in CD_3OD.

Changes in carbon hybridization resulting from the oxidation of hyperforin and ring closure to furohyperforin were clearly evident in the ^{13}C NMR spectra. The olefinic resonances at δ123.74 and δ134.25 belonging to C-32 and C-33 in hyperforin were absent in the spectrum of furohyperforin and replaced by the resonances at δ90.07 and δ70.84 of the corresponding sp^3 carbons indicating that C-32 and C-33 are attached to the oxygen.

The resonances belonging to C-6, C-7 and C-9 which were not observable in ^{13}C NMR spectrum of hyperforin due to fluxional keto-enol equilibrium, re-emerged as sharp signals at δ59.37, δ172.89 and δ192.69, respectively, in the spectrum of furohyperforin.

The ^{1}H and ^{13}C NMR spectrum of furohyperforin obtained in this study appeared to have better resolution than those previously reported. The vinylic protons reported as multiplets (Verotta et al., 2000) were resolved

Table 3
NMR data of furohyperforin and furoadhyperforin

Position	Furohyperforin			Furoadhyperforin		
	δ_H (J in Hz)	δ_C	HMBC	δ_H (J in Hz)	δ_C	HMBC
1	–	204.49	5, 31	–	204.49	5, 31
2	–	83.22	14, 15	–	83.26	14, 15
3	–	48.23	4, 5, 14, 15	–	48.28	5, 14, 15
4	1.62, *m*	43.26	3, 5, 14, 21	1.62, m	43.3	5, 14, 15, 21
5	2.01, *dd* (4.4, 13.5)	37.99	1, 3, 4, 6, 7, 21, 31	2.01, *dd* (4.3, 13.3)	38.02	1, 3, 4, 6, 7, 21, 31
	1.51, *t* (12.9)			1.51, *t* (13.0)		
6	–	59.37	5, 31	–	59.34	5, 31
7	–	172.89	5, 26, 31	–	172.90	5, 26, 31
8	–	116.64	26	–	116.60	26, 29, 30
9	–	192.69	26	–	192.83	26
10	–	209.47	11, 12, 13	–	209.04	11, 12, 13
11	1.98, *sept.* (6.5)	41.97	2, 10, 12, 13	1.74, *m*	48.71	10, 12, 13, 13′
12	1.09, *d* (6.5)	20.38	10, 11, 13	1.09, *d* (6.5)	16.62	10, 11, 13
13	1.00, *d* (6.5)	21.35	10, 11, 12	1.27, *m*	27.41	10, 11, 12, 13′
				1.69, *m*		
14	1.04, *s*	13.43	2, 3, 4, 15	1.05, *s*	13.35	2, 3, 4, 15
15	2.06, *m*	36.31	2, 3, 4, 14, 16, 17	2.07, *m*	36.39	2, 3, 4, 14, 16, 17
	1.32, *m*			1.32, *m*		2, 3, 4, 14, 16, 17
16	2.15, *m*	25.19	15, 17, 18	2.16, *m*	25.26	15, 17, 18
	1.93, *m*			1.92, m		3, 15, 17, 18
17	5.06, *br dd* (7.05, 13.49)	124.70	15, 16, 19, 20	5.06, *br t* (7.4)	124.7	15, 16, 19, 20
18	–	131.08	16, 19, 20	–	131.10	16, 19, 20
19	1.64, *s*	25.67	17, 18, 20	1.64, *s*	25.64	17, 18, 20
20	1.60, *s*	17.72	17, 18, 19	1.59, *s*	17.66	17, 18, 19
21	2.17, *m*	27.06	4, 5, 22, 23	2.17, *m*	27.08	4, 5, 22, 23
	1.77, *dd* (10.2, 23.2)		4, 5, 22, 23	1.77, *br m*		4, 5, 22, 23
22	4.94, *br t* (7.05)	122.25	4, 21, 24, 25	4.94, *br t* (7.1)	122.26	4, 21, 24, 25
23	–	133.50	21, 24, 25	–	133.49	21, 24, 25
24	1.70, *s*	25.89	22, 23, 25	1.69, *s*	25.89	22, 23, 25
25	1.57, *s*	17.95	22, 23, 24	1.57, *s*	17.95	22, 23, 24
26	3.14, *dd* (6.9, 14.2)	22.09	7, 8, 9, 27, 28	3.15, *dd* (6.9, 14.4)	22.16	7, 8, 9, 27, 28
	3.01, *dd* (7.6, 14.2)			3.01, *dd* (7.7, 14.4)		
27	5.07, *br dd* (7.05, 13.5)	121.15	8, 26, 29, 30	5.06, *br t* (7.4)	121.2	8, 26, 29, 30
28	–	132.51	26, 29, 30	–	132.38	26, 29, 30
29	1.65, *s*	25.6	27, 28, 30	1.64, *s*	25.67	27, 28, 30
30	1.69, *br s*	17.82	27, 28, 29	1.70, *s*	17.83	27, 28, 29
31	2.65, *dd* (10.8, 13.0)	30.16	1, 5, 6, 7, 32, 33	2.66, *dd* (10.8, 13.0)	30.23	1, 5, 6, 32, 33
			1, 5, 6, 32, 33	1.76, *dd* (5.6, 13.0)		
						1, 6, 7, 32, 33, 34
	1.76, *dd* (5.6, 13.0)					
32	4.55, *dd* (5.6, 10.8)	90.07	7, 31, 33, 34, 35	4.54, *dd* (5.6, 10.8)	90.08	7, 31, 33, 34, 35
33	–	70.84	31, 34, 35	–	70.83	31, 34, 35
34	1.38, *s*	26.88	32, 33, 35	1.38, *s*	26.91	32, 33, 35
35	1.21, *s*	24.0	32, 33, 34	1.22, *s*	24.04	32, 33, 34
13′				0.77, *t* (7.4)	11.54	11, 13

Measured at 600 MHz (^{1}H) and 150 MHz (^{13}C) in $CDCl_3$.

to a doublet of doublets (H-17) and triplet (H-22) while the 4 methyl groups (H-19 and H-29 and H-24 and H-30) reported as two broad singlets into 4 singlets. The chemical shifts of C-32 and C-33 resonances were reassigned to δ90.07 and δ70.84 (reversal of the assignment) from the HSQC and HMBC spectra.

2.3.3. Furoadhyperforin

Furoadhyperforin is a homologue of furohyperforin with an additional methyl group at the C-13 position (Table 3). The only difference between the NMR spectrum of furoadhyperforin and furohyperforin is the 2-butyl replacing C-10 isopropyl resonances. Apart from an additional triplet at δ0.77 of H-13′ characteristic of furoadhyperforin, the ^{1}H NMR spectrum of furoadhyperforin exhibited two multiplets centred at δ1.27 and δ1.69 (H-13) replacing the isopropyl methyl doublet at δ1.00 (H-13, $J = 6.5$ Hz) and a multiplet at δ1.74 replacing a septet at δ1.98 (H-11, $J = 6.5$ Hz) in furohyperforin.

The ^{13}C NMR spectra of furoadhyperforin showed an additional resonance at δ11.54 that corresponded to C-13′ and also minor changes in the chemical shift of C-11, C-12, and C-13 from furohyperforin induced by the presence of C-13′.

Table 4
NMR data of furohyperforin isomer 1 and furohyperforin isomer 2

Position	Furohyperforin isomer 1			Furohyperforin isomer 2		
	δ_H (J in Hz)	δ_C	HMBC	δ_H (J in Hz)	δ_C	HMBC
1	–	205.82		–	206.4	
2	–	83.65		–	84.23	
3	–	48.26		–	48.79	
4	1.57, *m*	43.08		1.67, *m*	42.89	
5	1.87, *dd* (3.8, 10.1)	37.66	1	1.93, *dd* (4.3, 13.6)	37.52	
	1.46, *t* (13.0)			1.44, *t* (13.0)		
6	–	54.7		–	54.8	
7	–	176.36		–	176.2	
8	–	118.29		–	119.2	
9	–	187.4		–	187.02	
10	–	209.34		–	209.76	
11	2.17, *sept.* (6.5)	42.10	10	2.12, *sept.* (6.5)	42.65	
12	1.12, *d* (6.5)	20.28	10, 11, 13	1.14, *d* (6.5)	20.88	10, 11, 13
13	1.05, *d* (6.5)	21.23	10, 11, 12	1.06, *d* (6.5)	21.87	10, 11, 12
14	1.01, *s*	13.46	2, 3, 4, 15	1.02, *s*	12.96	2, 3, 4
15	1.89, *m*	36.46		1.44, *m*	36.85	
	1.45, *m*					
16	2.10, *m*	24.70		2.11, *m*	26.88	
	1.88, *m*			1.80, *m*		
17	5.05, *br t* (6)	124.43	19, 20	4.96, *t* (7.1)	122.73	
18	–	130.94	19, 20	–	133.81	
19	1.64, *s*	25.46	17, 18, 20	1.71, *s*	25.0	17, 18, 20
20	1.59, *s*	17.50	17, 18, 19	1.58, *s*	17.04	17, 18, 19
21	2.10, *m*	26.98	1.86, *m*		35.55	
	1.74, *m*		1.54, *m*			
22	4.92, *t* (7.05)	122.24		5.05, *m*	124.90	
23	–	133.43		–	131.34	
24	1.68, *s*	25.84	22, 23, 25	1.65, *s*	24.76	22, 23, 25
25	1.55, *s*	17.64	22, 23, 24	1.60, *s*	16.79	22, 23, 24
26	2.98, *dd* (15, 10.5)	27.24		2.99, *dd* (14.7, 10.2)	25.96	
	2.86, *dd* (15, 8)			2.95, *dd* (14.7, 8.3)		
27	4.72, *dd* (10.5, 8)	92.25		4.81, *dd* (10.2, 8.3)	92.26	
28	–	71.95		–	72.17	
29	1.27, *s*	24.82	27, 28, 30	1.31, *s*	25.53	27, 28, 30
30	1.21, *s*	23.48	27, 28, 29	1.18, *s*	22.15	27, 28, 29
31	2.51, *dd* (14.5, 7)	28.82		2.51, *br dd* (14.7)	28.33	
	2.42, *dd* (14.5, 8)			2.47, *dd* (14.7, 8.9)		
32	5.07, *m*	118.09	34, 35	5.00, *m*	119.13	
33	–	134.64	34, 35	–	135.17	
34	1.67, *s*	25.56	32, 33, 35	1.70, *s*	24.8	
35	1.69, *s*	17.84	32, 33, 34	1.70, *s*	17.26	

Measured at 600 MHz (^{1}H) and 150 MHz (^{13}C) in $CDCl_3$.

2.3.4. Furohyperforin isomers 1 and 2

Furohyperforin isomers 1 and 2 (Table 4) are positional isomers of furohyperforin. It has been suggested that the furan ring in different positions in furohyperforins arose from the keto-enol tautomerism of hyperforin (Fuzzati et al., 2001).

The most significant differences between furohyperforin isomers 1 and 2, and furohyperforin (Tables 3 and 4) are the resonances belonging to the oxymethine and olefinic protons. Compared to furohyperforin, furohyperforin isomers 1 and 2 exhibited an upfield shift of H-26 to H-30 resonances (0.2–0.4 ppm) and a downfield shift of H-31 to H-35 resonances (0.14–0.67 ppm). This can be explained in terms of greater proton shielding on the furan ring than on the isoprenyl chain. The formation of the furan ring at C-7, C-8 position in furohyperforin isomer 1 and C-8, C-9 position in furohyperforin isomer 2 also resulted in the downfield shift of the isopropyl resonances (H-11, H-12 and H-13) by approximately 0.2–0.5 ppm.

The changes in ^{13}C resonances reflecting the alteration of carbon hybridization resulting from the different oxidative ring closures of the hyperforin prenyl chain at C-6 position for furohyperforin and at C-8 position for furohyperforin isomers 1 and 2 are clearly evident in the spectra.

Furohyperforin isomers are distinguished from furohyperforin by a large change in the ^{13}C chemical shift due to the changes in C-32, C-33, C-27, C-28 hybridization. In addition, minor changes were also observed in the chemical shift of C-26 and C-31 due to restricted rotation. Compared with the ^{13}C NMR spectrum of furohyperforin, the spectra of furohyperforin isomers showed sp^2 olefinic carbon resonances of C-32 and C-33 (δ118.09 and δ134.64

in isomer 1 and δ119.13 and δ135.17 in isomer 2) instead of the corresponding furohyperforin sp^3 carbon resonances (δ90.07 and δ70.84). The olefinic C-27 and C-28 carbon resonances (δ121.15 and δ132.51) in furohyperforin were replaced by the corresponding sp^3 carbon resonances (δ92.25 and δ71.95 in isomer 1 and δ92.26 and δ72.17 in isomer 2) in the spectra of furohyperforin isomers.

2.4. In vitro fluorometric recombinant CYP3A4 enzyme assay: CYP3A4 enzyme inhibition

Effects of hyperforin and its analogues on CYP3A4 enzyme activity were determined employing the dealkylation property of CYP3A4 enzyme. The positive control miconazole (Fig. 2a) inhibited CYP3A4 enzyme in this fluorometric recombinant CYP3A4 assay with an IC_{50} value of 0.16 μM. The IC_{50} of miconazole from this assay is similar to the value reported from the testosterone 6β-hydroxylase assay (0.1 μM, Di Marco et al., 2005) but considerably lower than the value reported from the erythromycin N-demethylase assay (0.85 μM, Riley et al., 2001). Hyperforin and its analogues were found to be potent inhibitors of CYP3A4 enzyme in fluorometric recombinant CYP3A4 assay (Fig. 2b–d). With an exception of furohyperforin (IC_{50} 1.3 μM, Fig. 2d), hyperforin (IC_{50} 0.63 μM, Fig. 2b) was less potent at inhibiting CYP3A4 enzyme activity than the oxidized analogues furoadhyperforin and furohyperforin isomer 1 (IC_{50} 0.072 and 0.079 μM, respectively, Fig. 2c) and furohyperforin isomer 2 (IC_{50} 0.23 μM, Fig. 2d).

Hyperforin (IC_{50} 0.63 μM) was approximately four times more potent at inhibiting recombinant CYP3A4 enzyme activity in the fluorometric assay (this study) than in the testosterone 6β-hydroxylase assay (IC_{50} 2.3 μM, Obach, 2000). False positive reading of the fluorescence is not likely to be the cause of the high potency observed in the fluorometric enzyme assay as intrinsic fluorescence or quenching of the test compound had been minimised by including the background fluorescence and the control readings in the calculation of inhibitory potency. Clevidipine is another CYP3A4 enzyme inhibitor exhibiting low potency in the testosterone 6β-hydroxylase assay. Clevidipine was reported to be 3.2 times higher in the midazolam assay (IC_{50} 2.6 μM) than testosterone assay in (IC_{50} 8.4 μM) (Zhang et al., 2006).

This study shows that oxidized acylphloroglucinols with an exception of furohyperforin are more potent than hyperforin at inhibiting CYP3A4 enzyme activity. Oxidized hyperforin derivatives have also been shown to be more potent as inhibitors of 5-lipoxygenase activity (0.04–0.9 μM) than hyperforin (IC_{50} 0.19 μM) (Feißt et al., 2005). In contrast, oxidized acylphloroglucinols ($IC_{50} > 20$ μM) were reported to be approximately 10 times less potent than hyperforin (IC_{50} 0.2 μM) at inhibiting synaptosomal reuptake of serotonin (Verotta et al., 2002). Taken together, these findings suggest that unlike serotonin reuptake inhibition, the β-dicarbonyl moiety of the reduced acylphloroglucinol hyperforin is not required for high inhibitory potency of 5-lipoxygenase and CYP3A4 enzyme activity.

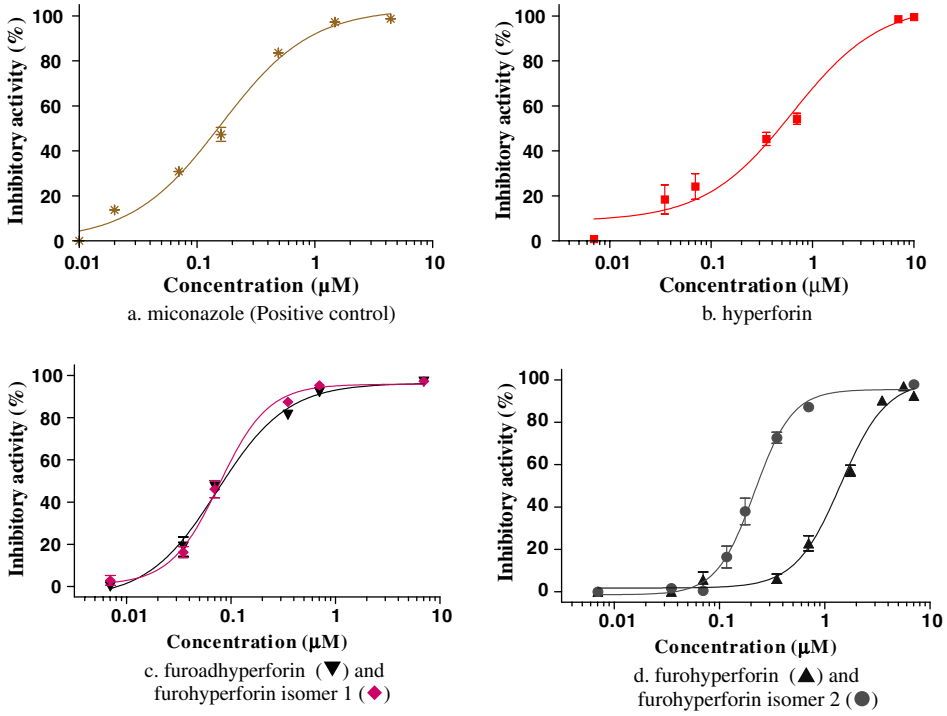

Fig. 2. Effects of hyperforin and its analogues on recombinant CYP3A4 enzyme. Miconazole (positive control, a), hyperforin (b), furoadhyperforin, furohyperforin isomer 1 (c), furohyperforin, furohyperforin isomer 2 (d) were tested over a range of concentrations 0.007 to 10 μM. Data presented as the means (±SEM) of three independent experiments each performed in duplicates.

Our study shows that acylphloroglucinols inhibit potently CYP3A4 enzyme activity. Thus, increased drug clearance by St. John's wort may be explained by increased enzyme expression. There are examples of CYP3A4 enzyme inhibitors including clevidipine, DPC 681 and aprepitant that also act as inducers of the enzyme. Clevidipine is a moderate CYP3A4 inhibitor (IC_{50} 8.4 μM, testosterone assay and 2.6 μM, midazolam assay) exhibited 7.3-fold induction of the enzyme at 100 μM (Zhang et al., 2006). DPC 681, a potent inhibitor of CYP3A4 enzyme (IC_{50} 0.039 μM, testosterone assay) was shown to be a strong inducer of the enzyme (3-fold increase at 20 μM) (Luo et al., 2003). Clinically, aprepitant has been shown to inhibit the enzyme activity when given at a shorter time course then induce the expression of the enzyme on a longer time course (Shadle et al., 2004).

Clinical herb–drug interaction of St. John's wort has been shown to be dose-dependent on hyperforin (Mueller et al., 2006; Madabushi et al., 2006). Furthermore, herb–drug interaction was not observed in patients taking a low-hyperforin St. John's wort extract (Arold et al., 2005). Hyperforin is a potent inhibitor of CYP3A4 enzyme activity (Obach, 2000; this study) and a strong inducer of the enzyme expression (Komoroski et al., 2004; Cantoni et al., 2003; Madabushi et al., 2006). The oxidised acylphloroglucinols of St. John's wort are potent inhibitors of CYP3A4 enzyme activity (this study). Further study is still required to determine their effects on the enzyme expression and their level of contribution to herb–drug interaction of St. John's wort.

3. Conclusions

This study shows that acylphloroglucinols of St. John's wort are potent inhibitors of CYP3A4 enzyme activity. Therefore, the role of acylphloroglucinols in herb–drug interaction of St. John's wort is unlikely to involve modulation of CYP3A4 enzyme activity but may involve induction of the enzyme expression.

4. Experimental

4.1. Materials

The flowering bud and bloom parts of St. John's wort (*Hypericum perforatum* L.) collected from Mt. Taylor, Canberra, ACT, Australia were separated from the stems and leaves, and frozen until further use. A voucher specimen was identified by an Identification Botanist, Barbara Wiecek at the Botanical Information Service at Royal Botanic Garden, Sydney and registered as 729998. The flowering tops of St. John's wort were homogenized in EtOH using a homogenizer (Yamato, Japan). Silica gel 60H for short column vacuum chromatography and TLC aluminium sheets silica gel 60 F_{254} were purchased from Merck. TLC plates were visualized by UVGL-58 mineral-light lamp, multiband UV-254/366 nm. Filter agent Celite®521 was obtained from Aldrich. Ethanol, diethyl ether, hexane, dichloromethane and methanol were purchased from APS (Asia Pacific Specialty) chemicals, and distilled prior to use for normal-phase short column vacuum chromatography.

Recombinant human microsomal cytochrome P450 3A4 isozyme (expressed in baculovirus infected insect cells), magnesium chloride hexahydrate, EDTA, miconazole, NADP, glucose 6-phosphate, glucose 6-phosphate dehydrogenase, and sodium citrate were purchased from Sigma–Aldrich Co. Tris base was purchased from BDH; potassium dihydrogen phosphate from Research Organics; dipotassium hydrogen phosphate from Mallinckrodt. Benzylfluorescein (2-(6-benzyloxy-3-oxo-(3H)-xanthen-9-yl)-benzoic acid) was synthesized in the laboratory and the structure confirmed by NMR and MS. Black clear bottom 96-well microtiter plate (Greiner) was purchased from Interpath services. Fluorescence was measured using POLAR star OPTIMA multi-detection reader with FLUO star software, BMG Labtechnologies.

4.2. Purification of hyperforin and its analogues

St. John's wort flowering tops (fresh or frozen, 1 kg) was homogenized in ethanol (3 L) and stirred at room temperature for 4 h. The mixture was filtered through the filter agent and evaporated under reduced pressure using the rotary evaporator (Büchi R-114 with waterbath B-480) at 37 °C to give the ethanol extract (28 g, 2.8% wet weight), which was then re-extracted with ether to give the ether extract (25 g, 2.5% wet weight).

Fractionation of the resulting ether extract (25 g) by short column silica gel vacuum chromatography (10 cm diam. × 7 cm) gave the first fraction (9 g, 0.9% wet weight), which was dissolved in dichloromethane and again subjected to purification by short column vacuum chromatography (10 cm diam. × 7 cm) employing a stepwise gradient solvent system (hexane:ether; 100:0, 100:10, 90:10, 80:10, 70:10, 60:10, 50:10, 40:10, 30:10, 20:10, 10:10, 200 mL each step). Pure hyperforin was eluted in the 70:10 fraction, whereas the more polar hyperforin analogues containing furohyperforin, furoadhyperforin furohyperforin isomers 1 and 2 eluted in the 40:10 fraction.

Furohyperforin, furoadhyperforin, furohyperforin isomers 1 and 2 were purified by short column vacuum chromatography employing a more refined stepwise gradient elution using hexane and dichloromethane. Furohyperforin was eluted with hexane:dichloromethane 10:70, furoadhyperforin 10:60 from a 5.5 cm diam. × 8 cm silica gel column. Furohyperforin isomer 1 was eluted with hexane:dichloromethane 10:90, furohyperforin isomer 2 with 10:80 from a 4 cm diam. × 9 cm silica gel column.

Hyperforin (2.2 g) and four analogues of hyperforin (11–84 mg) were isolated and purified from St. John's wort flowering tops using short column vacuum chromatography.

The isolated hyperforin which accounted for 0.22% wet weight of the flowering tops and 8% of the ethanol extract, was obtained pure as determined by TLC, ^{1}H and ^{13}C NMR. Hyperforin analogues consisting of furohyperforin (0.3%), furoadhyperforin (0.2%), furohyperforin isomer 1 (0.04%) and 2 (0.05%) together constituted 0.59% of the ethanol extract (0.016% wet weight of the flowering tops) were also isolated with high purity as determined by TLC, ^{1}H and ^{13}C NMR.

All isolation and purification processes were carried out under reduced light and all samples were kept under nitrogen at −20 °C to minimize oxidative decomposition by light and oxygen.

4.3. In vitro recombinant CYP3A4 enzyme assay

The CYP3A4 enzyme assay was carried out using fluorometric enzyme assays in a 96-well microtiter plate following the procedure described by Chauret and coworkers (1999) with some modifications. Benzylfluorescein (BF) was employed as the CYP3A4 fluorescent substrate instead of dibenzylfluorescein because of its improved solubility in the buffer. Test samples including the positive control miconazole were prepared in acetonitrile to give final concentrations over a range of 0.007–10 μM. Briefly, to each well of the microtiter plate was added NADP generating solution (96 μL, 1.3 mM $NADP^{+}$, 3.3 mM glucose 6-phosphate, 3.3 mM $MgCl_2 \cdot 6\,H_2O$, and 0.4 U/mL glucose 6-phosphate dehydrogenase in 50 mM KPO_4, pH 7.4) followed by 4 μL of the vehicle acetonitrile (control) and the test samples. The plate was covered and then incubated at 37 °C on an orbital shaker at 70 rpm for 10 min. Enzyme reaction was initiated by the addition of enzyme/substrate (E/S) mixture (100 μL, 0.5 pmol CYP3A4 enzyme and 2 μM benzylfluorescein). The plate was further incubated for 15 min, followed by the addition of the stop solution (100 μL, 4:1 acetonitrile: 0.5 M Tris base solution) to terminate the enzyme activity. Background reading was measured in a similar manner except for the E/S mixture (100 μL) which was added after the enzyme reaction was terminated.

The fluorescence of BF metabolite fluorescein was measured on a fluorescence plate reader with an excitation wavelength of 485 nm and an emission wavelength of 538 nm (Scheme 1). The effect of test compounds on CYP3A4 enzyme was calculated as the percentage of the enzyme activity. In this study, all constituents of St. John's wort examined inhibited the activity of CYP3A4 enzyme. These activities were expressed as percentage of inhibitory activity and calculated using the following equation,

$$\%\ \text{inhibitory activity} = [100 - \{(F_t - F_{tb}/F_c - F_{cb}) \times 100\}],$$

where F_t is the fluorescence of the test compound, F_{tb} the background fluorescence of the test compound, F_c the fluorescence of the control, and F_{cb} is the background fluorescence of the control.

4.4. Liquid chromatography-mass spectrometry

Liquid chromatography/electrospray ionization mass spectrometry (LC/ESI MS) analysis was performed on a Finnigan/ Mat TSQ 7000 LC-MS/MS instrument. The mass spectrophotometer was operated in positive-ion electrospray infusion mode and the full scans were acquired from *m/z* 110.0–1250.0 (scan time 2.5 s). The mobile phase was MeOH containing 0.1% dichloromethane and the sample solution was infused at 3 μL/min.

4.5. NMR spectroscopy

^{1}H and ^{13}C NMR spectra were acquired on a Bruker Avance 600 MHz NMR spectrometer operating at 600.13 MHz for ^{1}H and 150 MHz for ^{13}C, fitted with a 5 mm TBI probe. The samples were protected from light throughout the experimental procedures. Chemical shifts in the CD_3OD spectra were referenced to the residual methanol-d_4 (δ_H 3.31 and δ_C 49.0), and in the $CDCl_3$ spectra to the residual $CHCl_3$ (δ_H 7.26 and δ_C 77.0). ^{1}H 1D, ^{13}C 1D, COSY, TOCSY, ^{1}H–^{13}C HSQC and ^{1}H–^{13}C HMBC were carried out on all the samples (Braun et al., 1998). The following parameters were used: ^{1}H pulse width, 7.9 μs (90° pulse); spectral width, 3.6 kHz; acquisition time, 4.56 s; resolution, 0.11 Hz/pt; relaxation delay, 10 s.

4.6. Data analysis

The half-maximal inhibitory concentrations (IC_{50}) were calculated using non-linear regression analysis fitted with sigmoidal equations, GraphPad Prism 4.02.

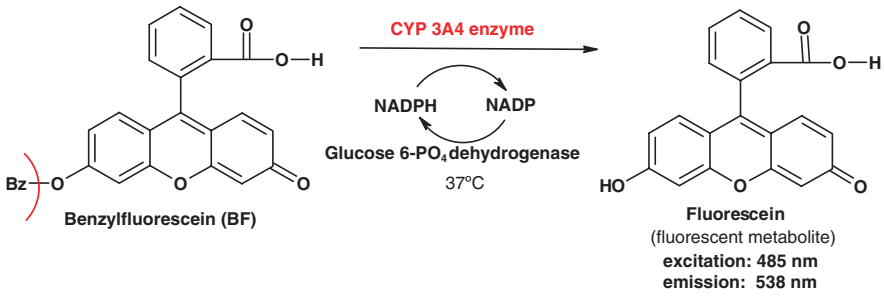

Scheme 1. Modulation of CYP3A4 enzyme activity by the test compounds is indicated by the oxidative de-alkylation of benzylfluorescein to fluorescein measured as the difference in the fluorescence intensity compared with the control.

Acknowledgments

We thank Mrs. Hilda Stender, NMR Facility, School of Chemistry, University of New South Wales for recording the NMR spectra and Mr. Bruce Tattam, Mass Spectrometry Analytical Facility, Faculty of Pharmacy, University of Sydney for recording the mass spectra. The award of Faculty of Pharmacy Elizabeth-Wunsch Scholarship, the University of Sydney International Postgraduate Award, and the Australian Department of Education, Science and Training International Postgraduate Research Scholarship is gratefully acknowledged.

Appendix A. Supplementary data

Supplementary data associated with this article can be found, in the online version, at doi:10.1016/j.phytochem.2006.09.018.

References

Arold, G., Donath, F., Maurer, A., Diefenbach, K., Bauer, S., Henneicke-von Zepelin, H.H., Friede, M., Roots, I., 2005. No relevant interaction with alprazolam, caffeine, tolbutamide, and digoxin by treatment with a low-hyperforin St. John's wort extract. Planta Med. 71 (4), 331–337.

Blumenthal, M., 2005. Herb sales down 7.4 percent in mainstream market. HerbalGram 66, 63.

Braun, S., Kalinowski, H.O., Berger, S., 1998. 150 and More Basic NMR Experiments. Wiley-VCH, Weinheim.

Breidenbach, T., Hoffmann, M.W., Becker, T., Schlitt, H., Klempnauer, J., 2000. Drug interaction of St. John's wort with cyclosporine. Lancet 335, 1912.

Butterweck, V., Christoffel, V., Nahrstedt, A., Petereit, F., Spengler, B., Winterhoff, H., 2003. Step by step removal of hyperforin and hypericin: activity profile of different *Hypericum* preparation in behavioral models. Life Sci. 73, 627–639.

Calapai, G., Crupi, A., Firenzuoli, F., Inferrero, G., Squadrito, F., Parisi, A., De Sarro, G., Caputi, A., 2001. Serotonin, norepinephrine and dopamine involvement in the antidepressant action of *Hypericum perforatum*. Pharmacopsychiatry 34 (2), 45–49.

Cantoni, L., Rozio, M., Mangolini, A., Hauri, L., Caccia, S., 2003. Hyperforin contributes to the hepatic CYP3A-inducing effect of *Hypericum perforatum* extract in the mouse. Toxicol. Sci. 75 (1), 25–30.

Chatterjee, S.S., Bhattacharya, S.K., Wonnemann, M., Singer, A., Müller, W.E., 1998. Hyperforin as a possible antidepressant component of *Hypericum* extracts. Life Sci. 63 (6), 499–510.

Chauret, N., Tremblay, N., Lackman, R.L., Gauthier, J.Y., Silva, J.M., Marois, J., Yergey, J.A., Nicoll-Griffith, D.A., 1999. Description of a 96-well plate assay to measure cytochrome P4503A inhibition in human liver microsome using a selective fluorescent probe. Anal. Biochem. 276, 215–226.

Cott, J.M., 1997. In vitro receptor binding and enzyme inhibition to *Hypericum perforatum* extract. Pharmacopsychiatry 30 (Suppl. 2), 108–112.

Cui, Y., Ang, C.Y.W., Beger, R.D., Heinze, T.M., Hu, L., Leakey, J., 2004. In vitro metabolism of hyperforin in rat liver microsomal systems. Drug Metab. Dispos. 32, 28–34.

Di Carlo, G., Borrelli, F., Ernst, E., Izzo, A.A., 2001. St. John's wort: Prozac from the plant kingdom. Trends Pharmacol. Sci. 22, 292–297.

Di Marco, A., Marcucci, I., Verdirame, M., Perez, J., Sanchez, M., Pelaez, F., Chaudhary, A., Laufer, R., 2005. Development and validation of a high-throughput radiometric CYP3A4/5 inhibition assay using tritiated testosterone. Drug Metab. Dispos. 33, 349–358.

Ernst, E., 1999. Second thoughts about safety of St. John's wort. Lancet 354, 2014–2016.

Feißt, C., Albert, D., Verotta, L., Werz, O., 2005. Evaluation of hyperforin analogues for inhibition of 5-lipoxygenase. Med. Chem. 1 (3), 287–291.

Fuzzati, N., Gabetta, B., Strepponi, I., Villa, F., 2001. High-performance liquid chromatography-electrospray ionisation mass spectrometry and multiple mass spectrometry studies of hyperforin degradation products. J. Chromatogr. A 926, 187–198.

Guengerich, F.P., 1997. Role of cytochrome P450 enzymes in drug–drug interactionsDrug–Drug Interactions: Scientific and Regulatory Perspectives. Academic Press, San Diego, pp. 7–35.

Hall, S., Wang, Z., Huang, S.M., Hamman, M.A., Vasavada, N., Adigun, A.Q., Hilligoss, J.K., Miller, M., Gorski, C., 2003. The interaction between St. John's wort and an oral contraceptive. Clin. Pharmacol. Ther. 74, 525–535.

Josey, E.S., Tackett, R.L., 1999. St. John's wort: a new alternative for depression. Int. J. Clin. Pharmacol. Ther. 37, 111–119.

Keller, J.-H., Karas, M., Müller, W.E., Volmer, D.A., Eckert, G.P., Tawab, M.A., Blume, H.H., Dingermann, T., Schubert-Zsilavecz, M., 2003. Determination of hyperforin in mouse brain by high-performance liquid chromatography/tandem mass spectrometry. Anal. Chem. 75, 6084–6088.

Komoroski, B.J., Zhang, S., Cai, H., Hutzler, M., Frye, R., Tracy, T.S., Storm, S.C., Lehmann, T., Ang, C.Y.W., Cui, Y., Venkataramanan, R., 2004. Induction and inhibition of cytochromes P450 by the St. John's wort constituent hyperforin in human hepatocyte cultures. Drug Metab. Dispos. 32 (5), 512–518.

Lawvere, S., Mahoney, M.C., 2005. St. John's wort. Complement. Altern. Med. 72 (11), 2249–2254.

Lecrubier, Y., Clerc, G., Didi, R., Kieser, M., 2002. Efficacy of St. John's wort extract WS 5570 in major depression: a double-blind, placebo-controlled trial. Am. J. Psychiatry 159 (8), 1361–1366.

Luo, G., Lin, J., Fiske, W.D., Dai, R., Yang, T.J., Kim, S., Sinz, M., Lecluyse, E., Solon, E., Brennan, J.M., Benedek, I.H., Jolley, S., Gilbert, D., Wang, L., Lee, F.W., Gan, L.-S., 2003. Concurrent induction and mechanism-based inactivation of CYP3A4 by an L-valinamide derivative. Drug Metab. Dispos. 31 (9), 1170–1175.

Madabushi, R., Frank, B., Drewelow, B., Derendorf, H., Butterweck, V., 2006. Hyperforin in St. John's wort drug interactions. Eur. J. Clin. Pharmacol. 62, 225–233.

Mai, I., Kruger, H., Budde, K., Johne, A., Brockmolleer, J., Neumayer, H.H., Roots, I., 2000. Hazardous pharmacokinetic interaction of St. John's wort (*Hypericum perforatum*) with the immunosuppressant cyclosporine. Int. J. Clin. Pharmacol. Ther. 38 (10), 500–502.

Maisenbacher, P., Kovar, K.A., 1992. Adhyperforin: a homologue of hyperforin from *Hypericum perforatum*. Planta Med. 58, 291–293.

Mannel, M., 2004. Drug interactions with St. John's wort: mechanism and clinical implications. Drug Safety 27 (11), 773–797.

Markowitz, J.S., Donovan, J.L., De Vane, C.L., Taylor, R.M., Ruan, Y., Wang, J.-S., Chavin, K.D., 2003. Effects of St. John's wort on drug metabolism by induction of cytochrome P450 3A4 enzyme. JAMA 290 (11), 1500–1504.

Mueller, S.C., Majcher-Peszynska, J., Uehleke, B., Klammt, S., Mundkowski, R.G., Miekisch, W., Sievers, H., Bauer, S., Frank, B., Kundt, G., Drewelow, B., 2006. The extent of induction of CYP3A by St. John's wort varies among products and is linked to hyperforin dose. Eur. J. Clin. Pharmacol. 62, 29–36.

Müller, W.E., 2003. Current St. John's wort research from mode of action to clinical efficacy. Pharmacol. Res. 47, 101–109.

Nahrstedt, A., Butterweck, V., 1997. Biologically active and other chemical constituents of the herb of *Hypericum perforatum* L. Pharmacopsychiatry 30S, 129–134.

Obach, R.S., 2000. Inhibition of human cytochrome P450 enzymes by constituents of St. John's wort, an herbal preparation used in the treatment of depression. J. Pharmacol. Exp. Ther. 294, 88–95.

Orth, H.C.J., Rentel, C., Schmidt, P.C., 1999. Isolation, purity analysis and stability of hyperforin as a standard material form *Hypericum perforatum* L. J. Pharm. Pharmacol. 51, 193–200.

Piscitelli, S.C., Brustein, A.H., Chairr, D., Alfaro, R.M., Falloon, J., 2000. Indinavir concentrations and St. John's wort. Lancet 355, 547–548.

Riley, R.J., Parker, A.J., Trigg, S., Manners, C.N., 2001. Development of a generalized, quantitative physicochemical model of CYP3A4 inhibition for use in early drug discovery. Pharmceut. Res. 18 (5), 652–655.

Roby, C.A., Anderson, G.D., Kantor, E., Dryer, D.A., Burstein, A.H., 2000. St. John's wort: effect on CYP3A4 activity. Clin. Pharmacol. Ther. 67, 451–457.

Schrader, E., 2000. Equivalence of St. John's wort extract (Ze 117) and fluoxetine: a randomised, controlled study in mild-moderated depression. Int. Clin. Psychopharmcol. 15, 61–68.

Schulz, V., 2006. Safety of St. John's wort extract compared to synthetic antidepressants. Phytomedicine 13, 199–204.

Shadle, C.R., Lee, Y., Majumdar, A.K., Petty, K.J., Gargano, C., Bradstreet, T.E., Evans, J.K., Blum, R.A., 2004. Evaluation of potential inductive effects of aprepitant on cytochrome P450 3A4 and 2C9 activity. J. Clin. Pharmcol. 44 (3), 215–223.

Verotta, L., Appendino, G., Bello, E., Jakupovic, J., Bombardelli, E., 1999. Furohyperforin, a prenylated phloroglucinol from St. John's wort (*Hypericum perforatum*). J. Nat. Prod. 62, 770–772.

Verotta, L., Appendino, G., Jakupovic, J., Bombardelli, E., 2000. Hyperforin analogues from St. John's wort (*Hypericum perforatum*). J. Nat. Prod. 63, 412–415.

Verotta, L., Appendino, G., Belloro, E., Bianchi, F., Sterner, O., Lovati, M., Bombardelli, E., 2002. Synthesis and biological evaluation of hyperforin analogues. Part I. Modification of the enolized cyclohexanedione moiety. J. Nat. Prod. 65 (4), 433–438.

Verotta, L., 2003. *Hypericum perforatum*, a source of neuroactive lead structures. Curr. Top. Med. Chem. 3, 187–201.

Vugdelija, S., Vajs, V., Trifunovic, S., Djokovic, D., Milosavljevic, S., 2000. A new heterocyclization product of adhyperforin from *Hypericum perforatum* (St. John's wort). Molecules 5, M158.

Wang, Z., Ashraf-Khorassani, M., Taylor, L.T., 2004. Air/light-free hyphenated extraction/analysis system: supercritical fluid extraction on-line coupled with liquid chromatography-UV absorbance/electrospray mass spectrometry for the determination of hyperforin and its degradation products in *Hypericum perforatum*. Anal. Chem. 76 (22), 6771–6776.

Wang, Z., Gorski, C., Hamman, M., Huang, S.M., Lesko, L.J., Hall, S.D., 2001. The effects of St. John's wort (*Hypericum perforatum*) on human cytochrome P450 activity. Clin. Pharmacol. Ther. 70, 317–326.

Woelk, H., 2000. Comparison of St. John's wort and imipramine for treating depression: randomised controlled trial. Brit. Med. J. 321 (7260), 536–539.

Wolfender, J.L., Verotta, L., Belvisi, L., Fuzzati, N., Hostettmann, K., 2003. Structural investigations of isomeric oxidised forms of hyperforin by HPLC-NMR and HPLC-MS. Phytochem. Anal. 14, 290–297.

Zhang, J.G., Dehal, S.S., Ho, T., Johnson, D.M., Wong, J., 2006. Human cytochrome P450 induction and inhibition potential of clevidipine and its primary metabolite H152/81. Drug Metab. Dispos. 34 (5), 734–737.